Supplementary information

Elevated concentration of MoS_2 lowers efficacy of liquid-phase exfoliation and triggers production of MoO_x nanoparticles

Michal Bodík*[a], Adriana Annušová[a,b], Jakub Hagara[a], Matej Mičušík[c], Mária Omastová[c], Mário Kotlár[d], Juraj Chlpík[e], Julius Cirák[e], Helena Švajdlenková[c], Michal Anguš[f], Alicia Marín Roldán[f], Pavel Veis[f], Matej Jergel[a], Eva Majkova[a,b], and Peter Šiffalovič[a,b]

[a] Institute of Physics, Slovak Academy of Sciences, Dubravska cesta 9, 845 11 Bratislava, Slovakia
[b] Centre of Excellence for Advanced Materials Application, Dubravska cesta 9, 845 11 Bratislava, Slovakia
[c] Polymer Institute, Slovak Academy of Sciences, Dubravska cesta 9, 845 41 Bratislava, Slovakia
[d] Slovak University of Technology, University Science Park Bratislava Centre, Vazovova 5, 812 43 Bratislava, Slovakia
[e] Faculty of Electrical Engineering and Information Technology, Slovak University of Technology in Bratislava, Ilkovicova 3, 812 19 Bratislava, Slovakia
[f] Faculty of Mathematics, Physics and Informatics, Comenius University, Mlynska dolina F1, 842 48 Bratislava, Slovakia

* corresponding author: Michal.Bodik@savba.sk

Contents

Absorbance

The UV-Vis-NIR absorbance measurements were performed using an integral sphere in order to include the absorbed and scattered radiation as well. The samples were filled into a clean quartz cuvette with 1 cm light path. The baseline correction was performed by placing two identical quartz cuvettes filled with 45% ethanol solutions in the reference and sample beams. During the measurements, we always kept the 45% ethanol solution in the reference beam. The absorbance spectra of the samples with different initial MoS_2 concentrations are shown in Fig. S1.

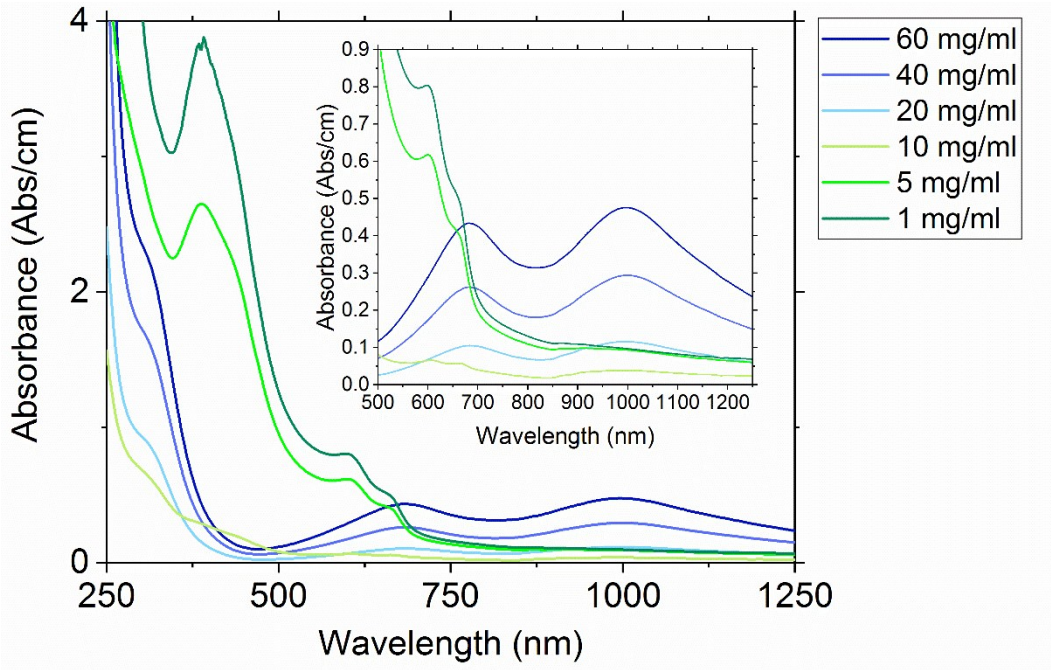

Fig. S1: The absorbance spectra of LPE MoS_2 at different initial concentrations. The inset shows the NIR part of the spectra with scaled absorbance axis.

The absorbance spectra of LPE MoO_2 and MoO_3 nanoparticles (Fig. S2) show similar characteristics in NIR region as the MoO_x prepared by LPE from MoS_2. In particular, MoO_2 exhibits similar peaks at approx. 700 nm and 1 000 nm. However, an additional new peak at 800 nm is present in the case of MoO_2.

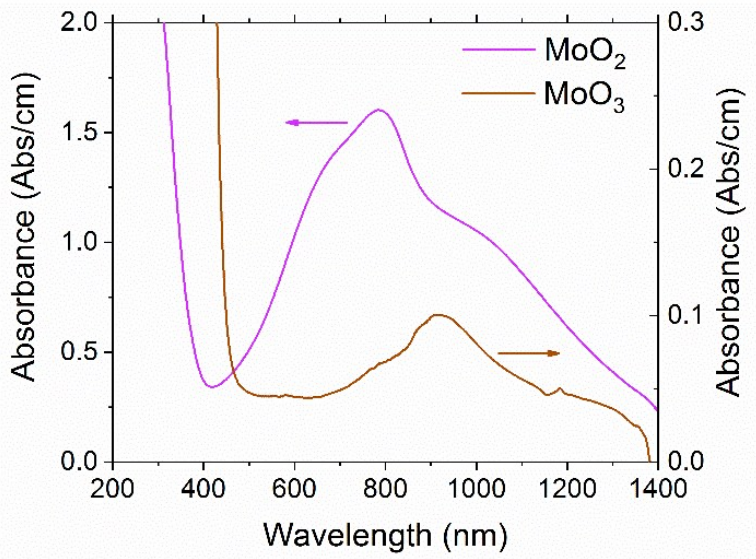

Fig. S2: The absorbance spectra of the MoO_2 and MoO_3 samples prepared by LPE at 60 mg/ml concentration.

In rare cases, the LPE initiated oxidation of MoS_2 resulted in different absorbance spectra. The third peak at approx. 800 nm appeared, similar to the one observed in MoO_2 absorbance spectrum (Fig. S3). Throughout the experiments, the integral intensity of the 800 nm peak varied. This suggests that the resulting oxides were not always identical.

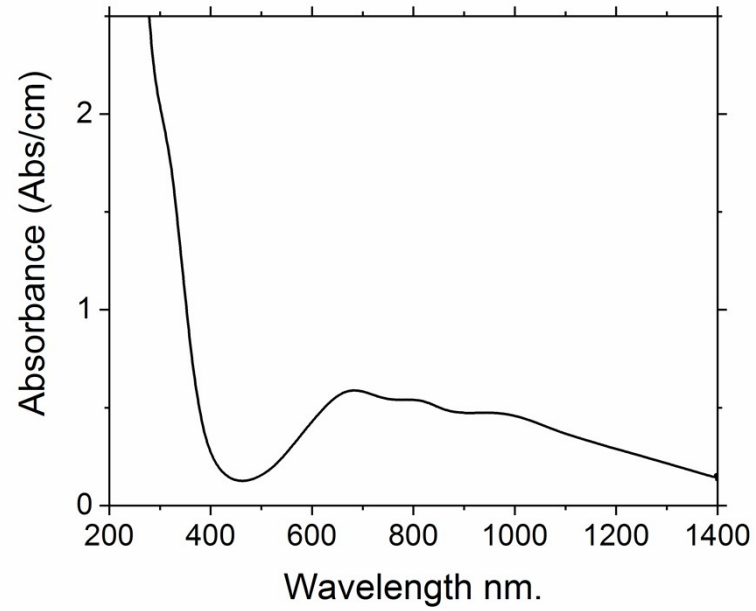

Fig. S3: The absorbance of the sample prepared by LPE at 60 mg/ml concentration of MoS_2.

Photoluminescence

The photoluminescence (PL) spectra of LPE MoS_2 at different initial concentrations were measured with an excitation wavelength of 355 nm. In the first step, we found the PL maximum excited at 355 nm (Fig. S4). Then the PL excitation (PLE) spectra were measured at a fixed detection wavelength of 433 nm, which corresponds to the PL maximum excited at 355 nm (Fig. S5). Contrarily, the LPE MoO_2 and MoO_3 nanoparticles exhibited no PL as it is visible from the excitation spectra (Fig. S5). A second series of PL spectra were measured with the excitation at 317 nm and subsequently self-consistently normalized using the Raman peak of water (Fig. S6).

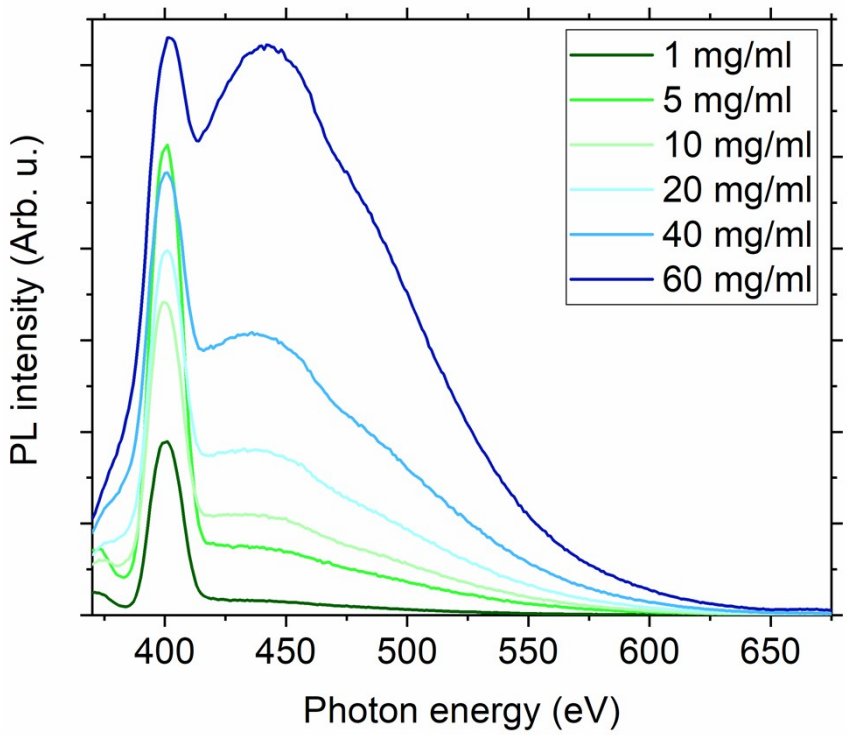

Fig. S4: The PL spectra measured with an excitation wavelength of 355 nm.

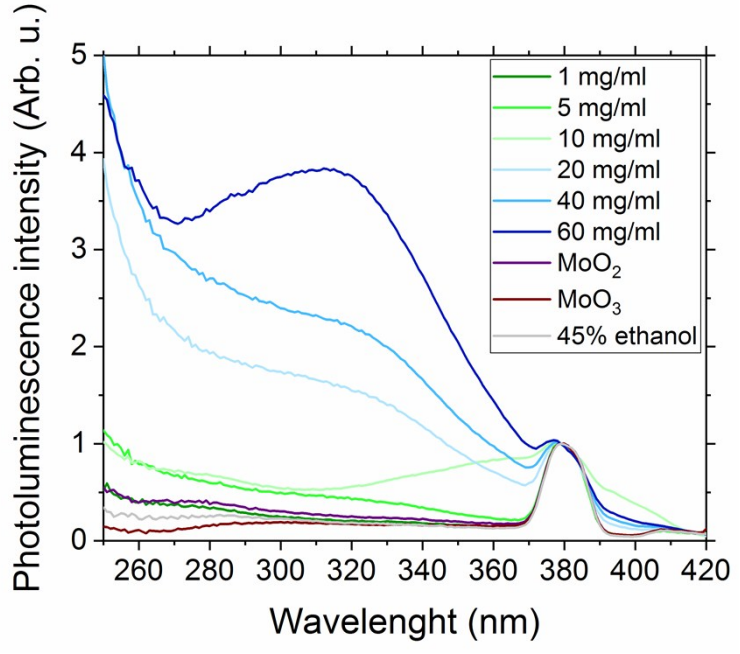

Fig. S5: The PLE spectra measured at the emission wavelength fixed at 433 nm.

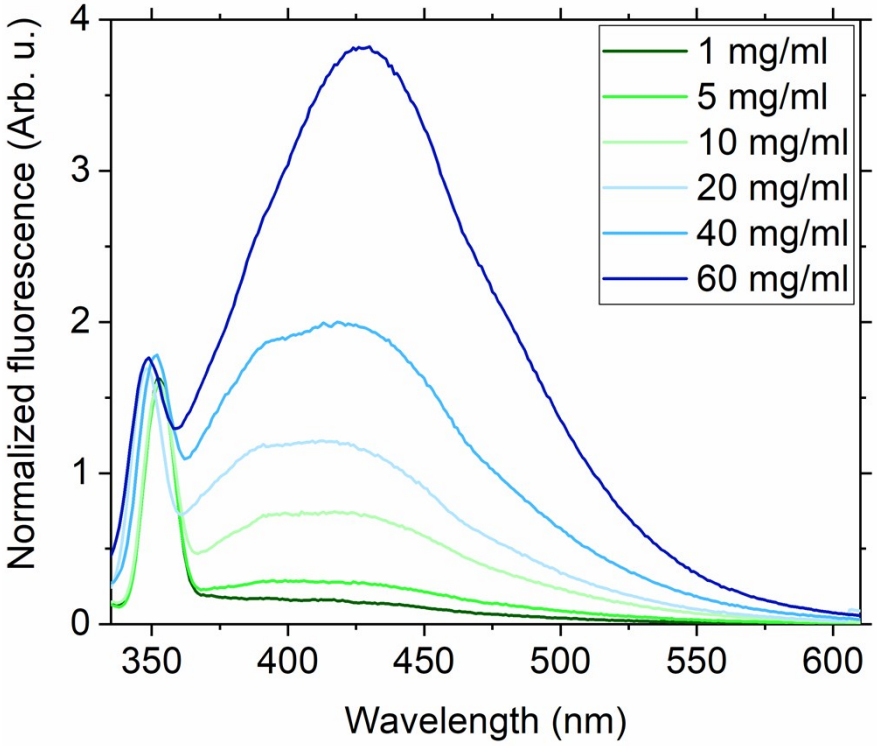

Fig. S6: The normalized PL emission with the excitation wavelength at 317 nm.

Raman spectroscopy

The Raman spectroscopy was performed in solution using an immersive objective. The objective was carefully cleaned with ethanol before each measurement to exclude possible cross-contamination. The integration time was set to 10 s for each sample. The power of excitation laser at 532 nm line was set to 2 mW. The Raman spectra shown in Fig. S7 confirm the decrease of MoS_2 Raman modes with the increasing initial MoS_2 concentrations. For the concentrations higher than 10 mg/ml only the Raman peaks of ethanol are present in the spectra.

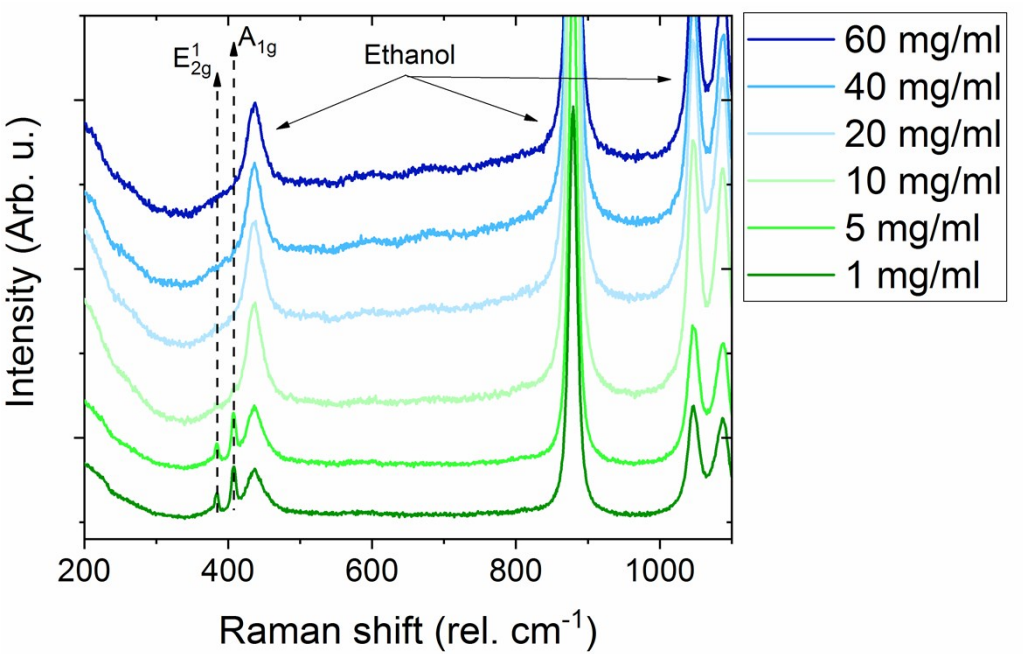

Fig. S7: Raman spectra of LPE samples with increasing initial MoS_2 concentration.

On the other hand, the Raman spectra of MoO_2 (Fig. S8a) and MoO_3 (Fig. S8b) LPE solutions exhibited a weak peak at 820 rel. cm^{-1}, that can be assigned to the α-MoO_3 phase. The MoO_3 solution showed additional weak peaks at approx. 1000 rel. cm^{-1} and 290 rel. cm^{-1}. Surprisingly, the MoO_2 solution did not show any peak corresponding to MoO_2 phase.

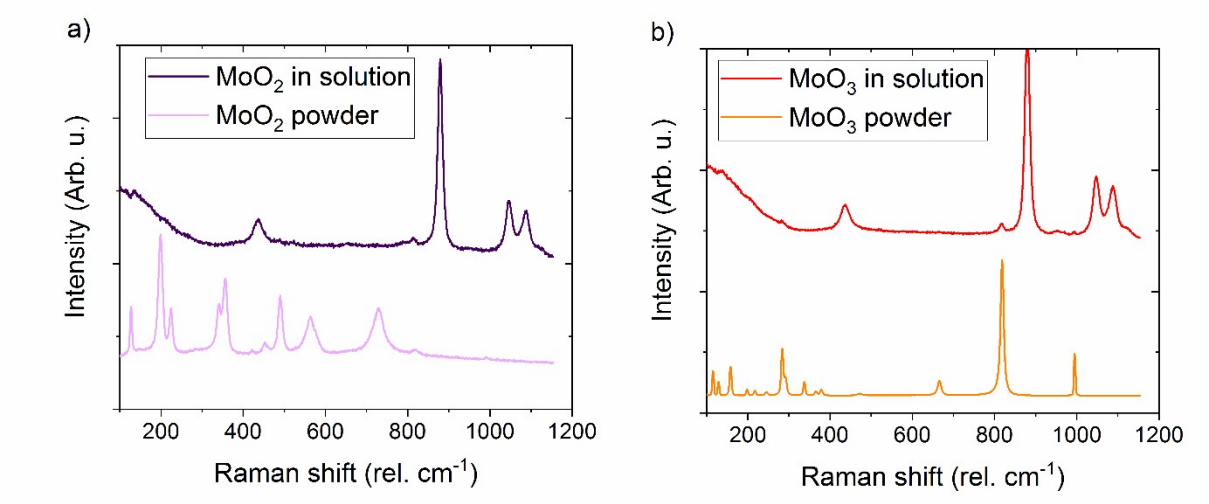

Fig. S8: The Raman spectra of pristine powders and the corresponding LPE solutions for a) MoO_2 and b) MoO_3.

XPS analysis

The high-resolution Mo 3d XPS spectrum of the sample prepared from the initial MoS_2 concentration of 1 mg/ml is shown in Fig. S9. No core-level shifts belonging to Mo oxides are visible in XPS spectrum. With the increase of initial MoS_2 concentration, new peaks corresponding to Mo^{5+}, Mo^{6+} and SO_3 states appeared (Fig. S10 – S14). The processed MoO_2 and MoO_3 powders contained only Mo^{5+} and Mo^{6+} bonded electrons in the Mo 3d shell (Fig. S15 – S16). A detailed composition of the samples is given in Table S1.

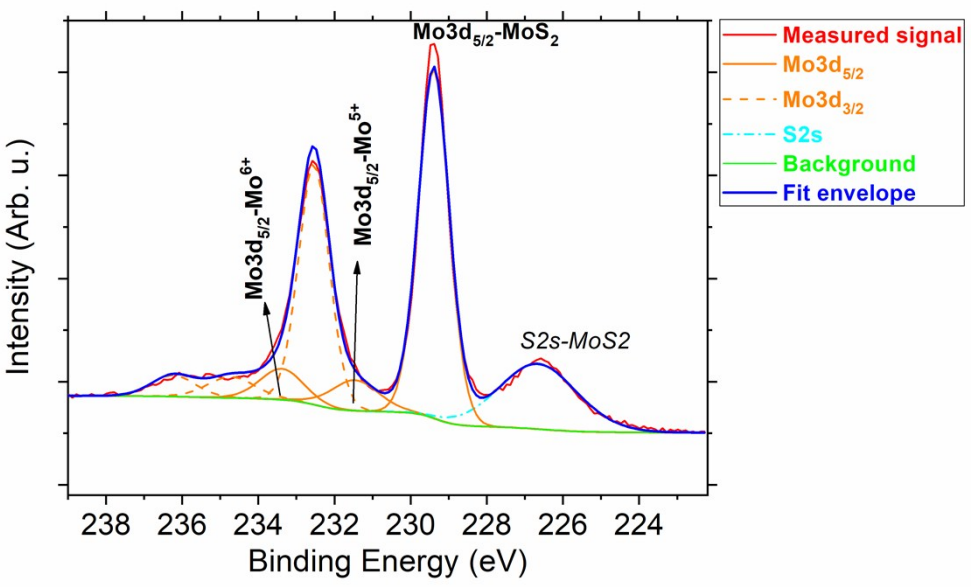

Fig. S9: The high-resolution XPS spectrum of the sample prepared from 1 mg/ml initial concentration of MoS_2.

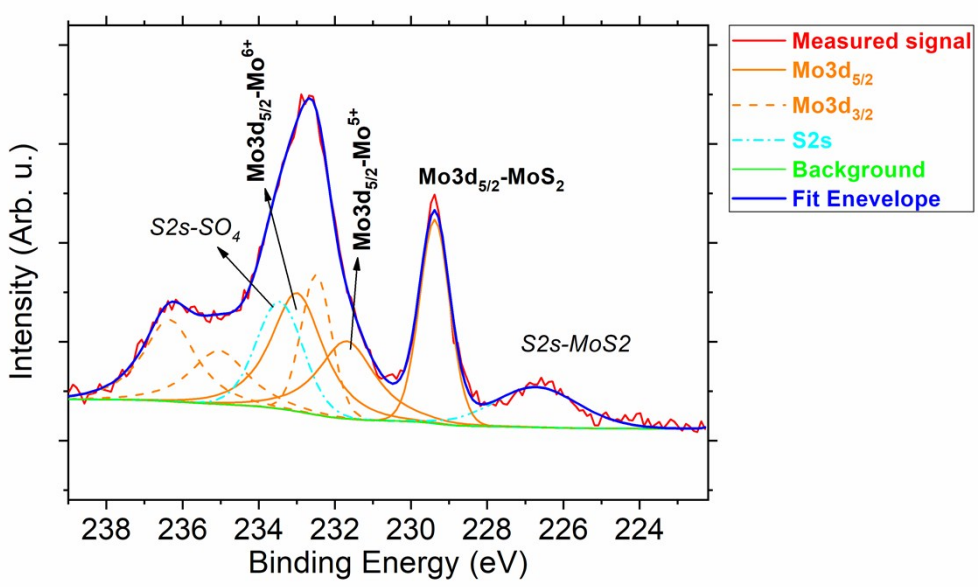

Fig. S10: The high-resolution XPS spectrum of the sample prepared from 5 mg/ml initial concentration of MoS_2.

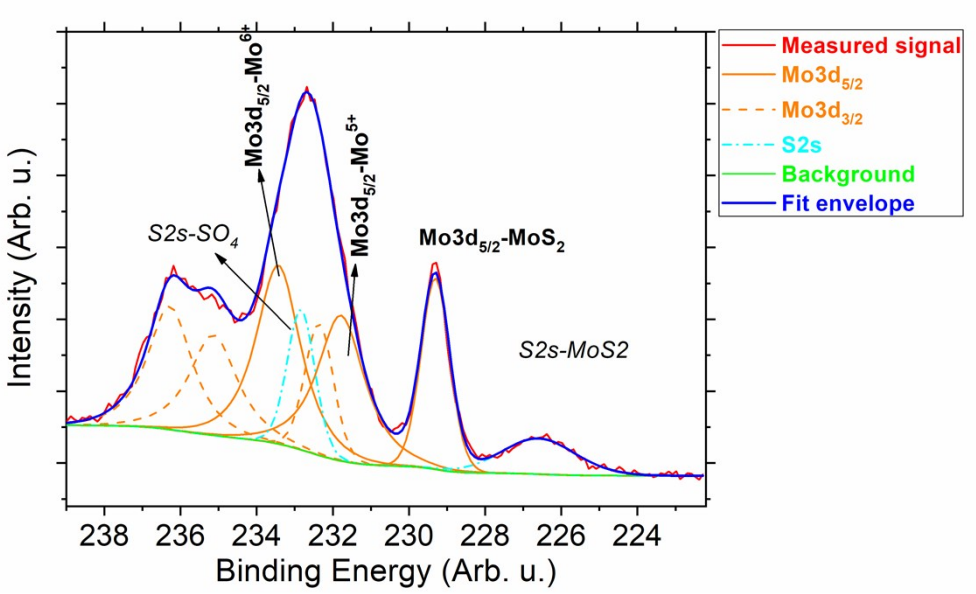

Fig. S11: The high-resolution XPS spectrum of the sample prepared from 10 mg/ml initial concentration of MoS_2.

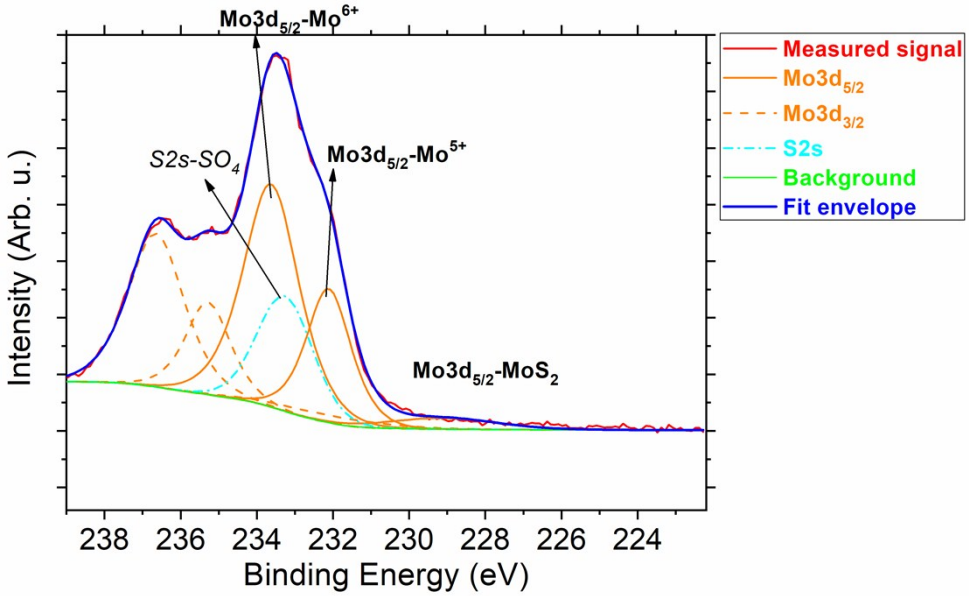

Fig. S12: The high-resolution XPS spectrum of the sample prepared from 20 mg/ml initial concentration of MoS_2.

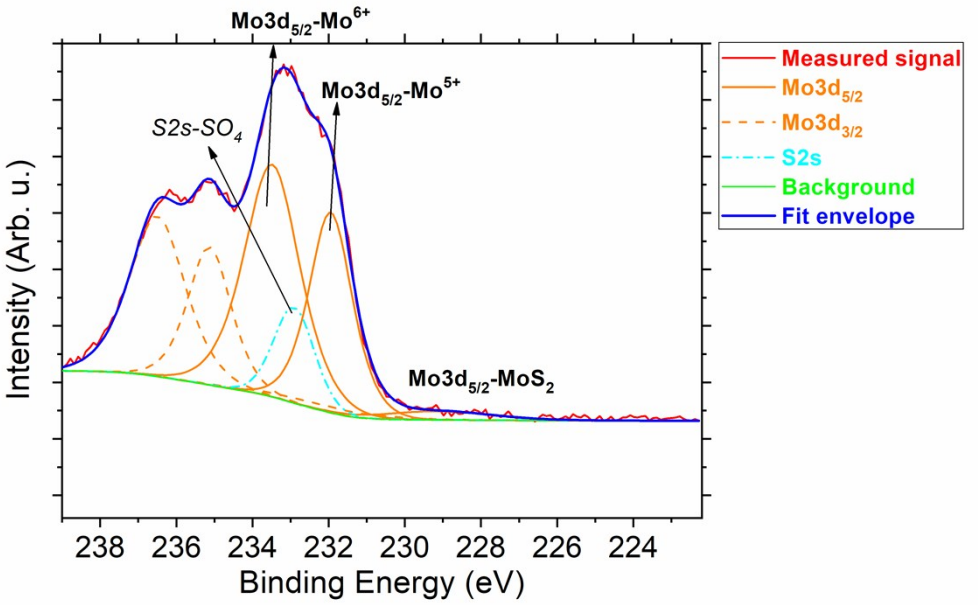

Fig. S13: The high-resolution XPS spectrum of the sample prepared from 40 mg/ml initial concentration of MoS_2.

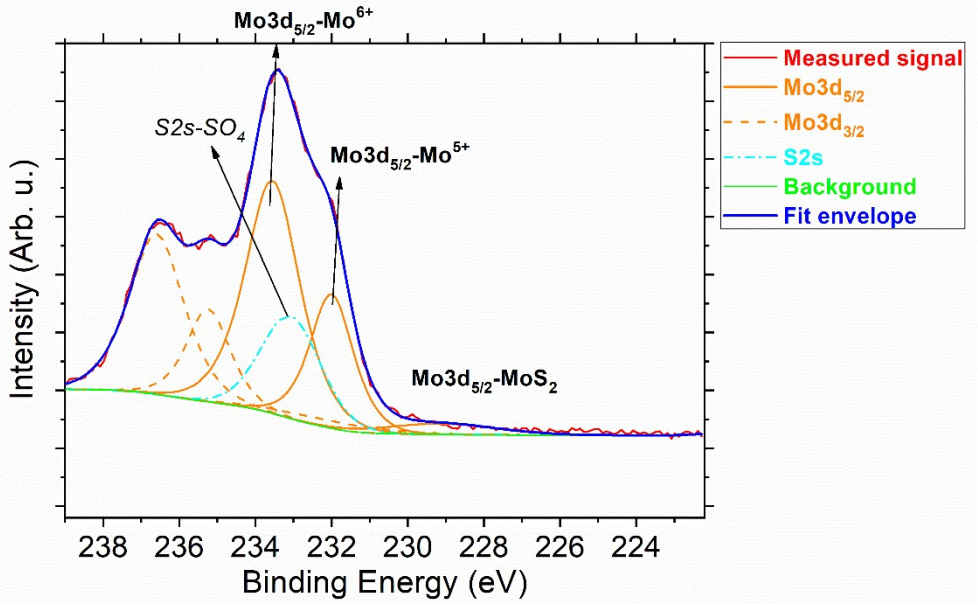

Fig. S14: The high-resolution XPS spectrum of the sample prepared from 60 mg/ml initial concentration of MoS_2.

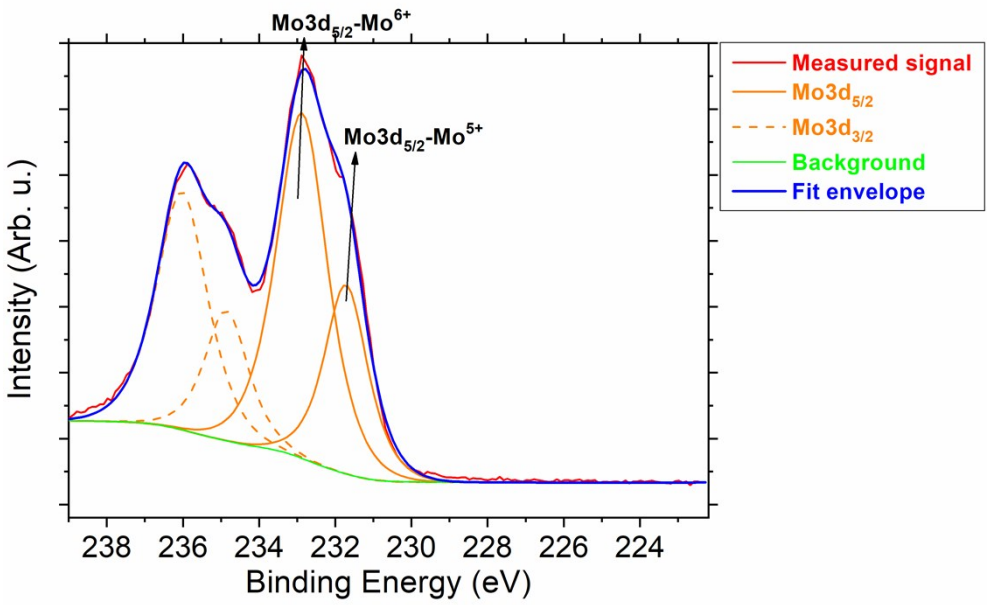

Fig. S15: The high-resolution XPS spectrum of the sample prepared from 60 mg/ml initial concentration of MoO_2.

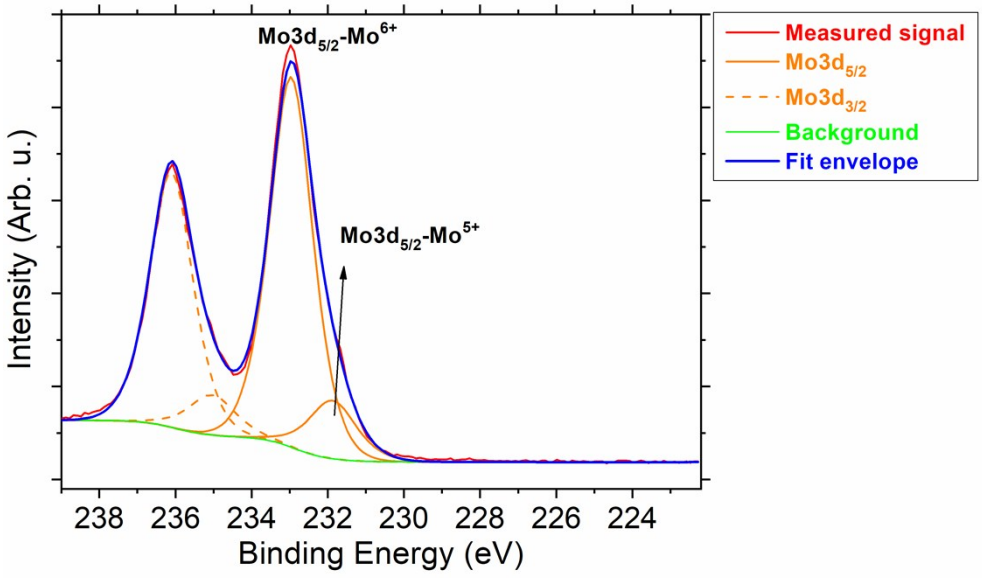

Fig. S16: The high-resolution XPS spectrum of the sample prepared from 60 mg/ml initial concentration of MoO_3.

Table 1: Detailed surface chemical composition of MoO_x samples.

Sample	Surface chemical composition [at.%]				
	Mo3d $MoS_2/Mo^{5+}/Mo^{6+}$ *229.4/231.7/232.6*	S2p MoS_2/S-O/SO_3 *162.3/165.8/168.9*	O1s MoO_x /C=O/C-O	C1s C-C/C-O/C=O/OC=O	Si2p
MoO_2	—/4.5/9.6	—	38.4/6.8/4.5	18.2/14.5/2.4/1.1	—
MoO_3	—/2.0/11.5	—	35.2/4.4/4.2	27.4/11.3/2.3/1.7	—
1mg/ml	6.9/0.9/0.9	15.5/1.8/5.3	3.3/19.2/8.1	13.9/3.1/1.8/1.0	18.4
5mg/ml	0.8/0.7/0.9	2.4/2.4/9.4	3.4/36.0/8.0	5.1/1.8/1.3/0.8	27.0
10mg/ml	1.0/1.5/1.7	2.7/1.7/7.5	9.8/27.5/7.1	16.5/2.7/0.9/1.0	18.4
20mg/ml	0.3/1.6/3.2	0.1/0.3/13.0	11.5/34.4/16.0	16.1/0.7/1.9/1.1	—
40mg/ml	0.2/2.2/3.3	0.3/0.8/8.7	13.3/27.7/11.5	18.1/4.7/0.9/1.2	7.1
60mg/ml	0.3/1.5/3.2	0.2/0.5/10.9	13.0/27.4/13.8	19.4/3.5/1.0/1.3	4.2

LIBS analysis

The surface-assisted Laser Induced Breakdown Spectroscopy (LIBS) measurements were performed in a vacuum chamber under Ar atmosphere at 10 Torr to determine the decrease of the concentration of sulfur. The solution of MoS_2 was dropped on a pure cleaned Al substrates. Simulated LIBS spectra using the NIST LIBS web application show that the S I-III lines are dominant in the VUV spectral range. Thus, enlarging the spectral down to the VUV region, it is possible to detect sulfur lines at our current experimental conditions (T_e ~ 1.21 eV and $n_e \sim 3 \cdot 10^{17}$ cm^{-3}) [Figure 2 at ref. 51 from main text]. We focused on the sulfur lines in the vacuum UV region (140 nm – 200 nm), showing the spectral lines S I at 129.57 nm and 131.02 nm, and O I at 130.22 nm, 130.49 nm and 130.60 nm (Fig. S17); and S I lines at 180.73 nm and 182.03 nm, and Al II lines at 181.84 nm, 181.93 nm and 182.01 nm (Fig. S18).

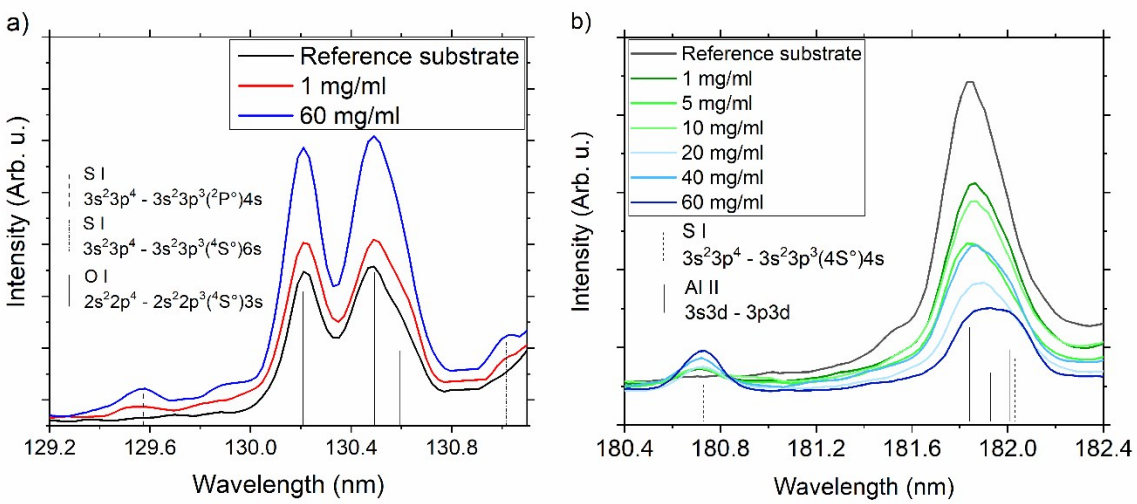

Fig. S17: Vacuum UV LIBS spectra for samples prepared from different initial concentrations for a) for S I at 129.57 nm and 131.02 nm, and O I at 130.22 nm, 130.49 nm and 130.60 nm, and b) S I lines at 180.73 nm and 182.03 nm, and Al II lines at 181.84 nm, 181.93 nm and 182.01 nm.

GIWAXS and GIXRD analysis

Fig. S18 and Fig. S19 show the GIWAXS patterns of LPE samples prepared from MoO_2 and MoO_3 powders, respectively. Neither of them shows an oriented MoO_x phase (compare to Fig. 6b in the main text).

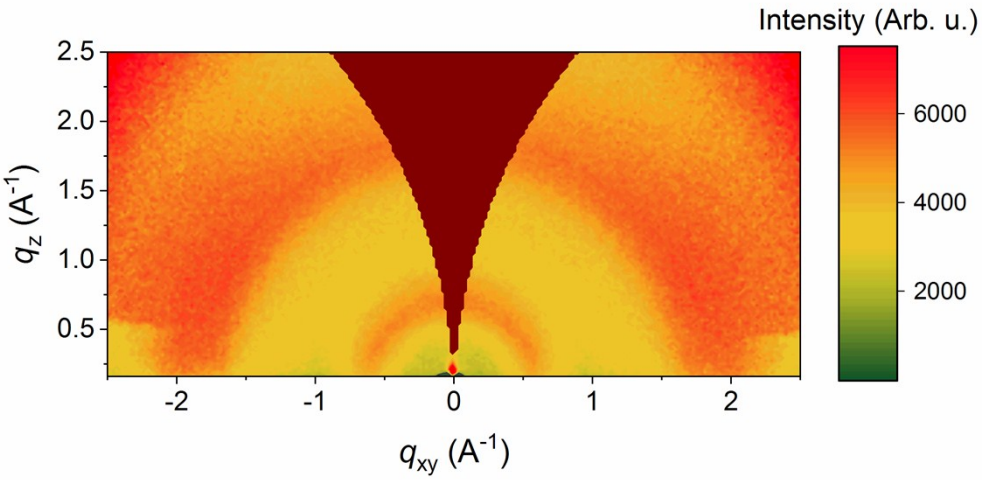

Fig. S18: GIWAXS pattern of the sample prepared from 60 mg/ml initial concentration of MoO_2.

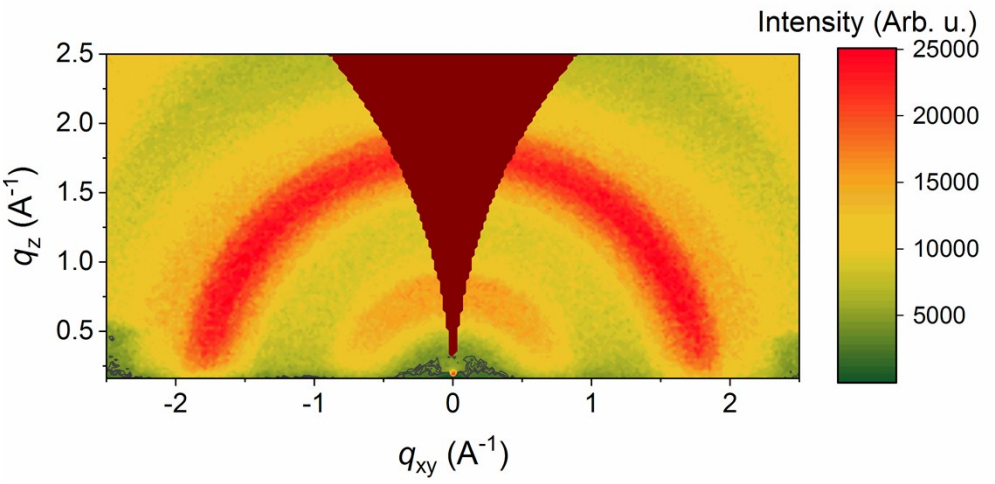

Fig. S19: GIWAXS pattern of the sample prepared from 60 mg/ml initial concentration of MoO_3.

In order to further study the evolution of different MoO_x phases, we performed complementary GIXRD measurements (angle of incidence 1°) with varying initial MoS_2 concentrations (Fig. S20). The samples prepared from the initial concentrations of 1, 5 and 10 mg/ml display only 002 diffraction peak ($2\theta = 14.4°$) of MoS_2 phase. For the concentrations above 10 mg/ml, new peaks were observed in GIXRD spectra coming from a variety of MoOx phases with oxygen-deficient stoichiometry. These peaks can be assigned e.g. to Mo_4O_{11}, $Mo_{17}O_{47}$, Mo_9O_{26} and χMo_8O_{23} phases.

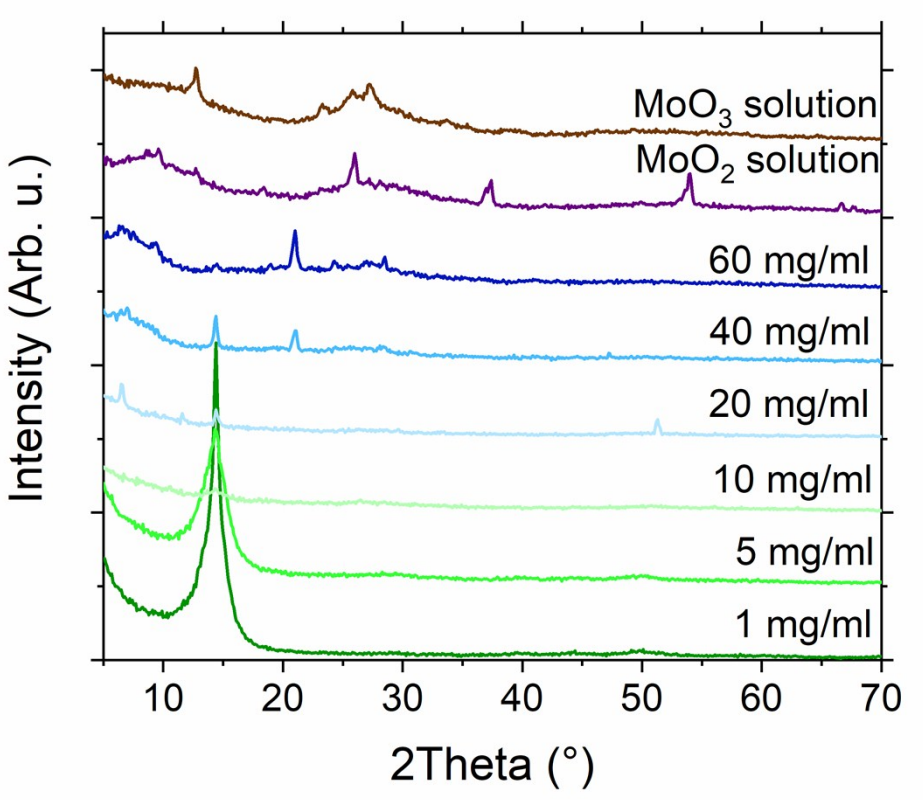

Fig. S20: GIXRD patterns of all LPE samples prepared from MoS_2, MoO_2 and MoO_3 powders.

TEM and EDS

TEM revealed a high dispersion in the size of nanoparticles exfoliated from an initial MoS_2 concentration of 60 mg/ml. The TEM micrographs confirm the presence of smaller (Fig. S21) as well as larger nanoparticles (Fig. S22). The observed two classes of nanoparticles may differ in stoichiometry. In order to provide evidence for this, the size-exclusion chromatography would be a suitable separation technique. However, this goes beyond the scope of this study. The EDS measurements shown in Fig. S23 confirmed, that the nanoparticles contain Mo atoms. However, the overlap of Mo (2.29 eV) and S (2.31 eV) signals prevented a more exact evaluation of the Mo/S ratio.

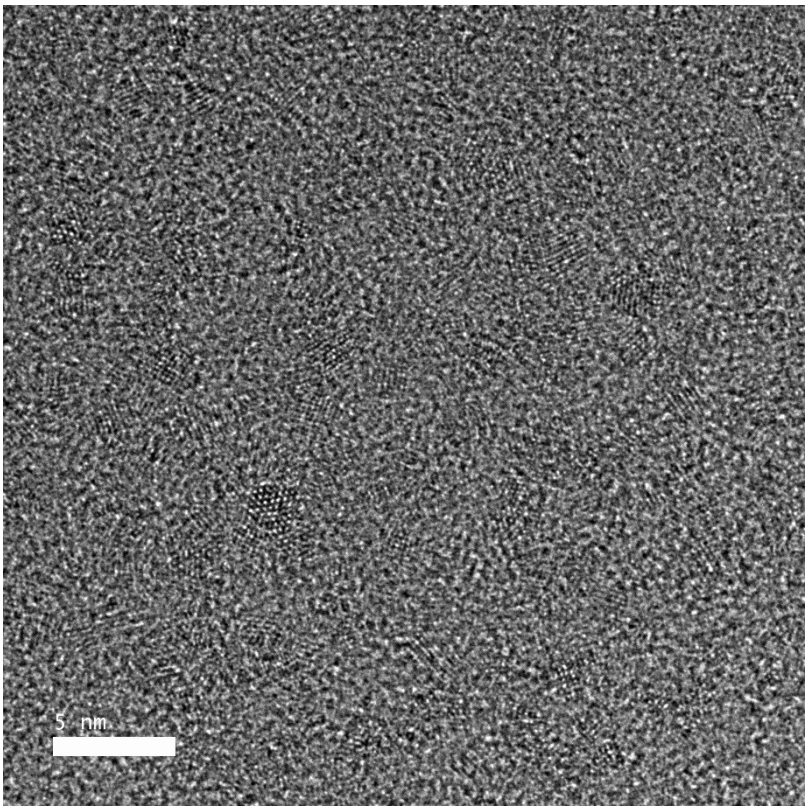

Fig. S21: TEM image of the area containing smaller MoO_x particles.

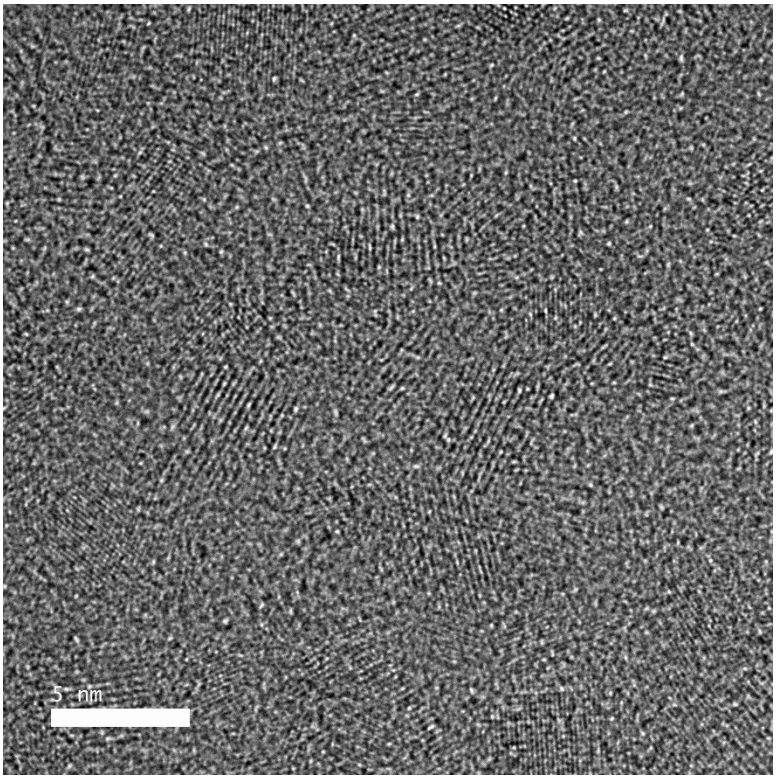

Fig. S22: TEM image of the area containing larger MoO_x particles.

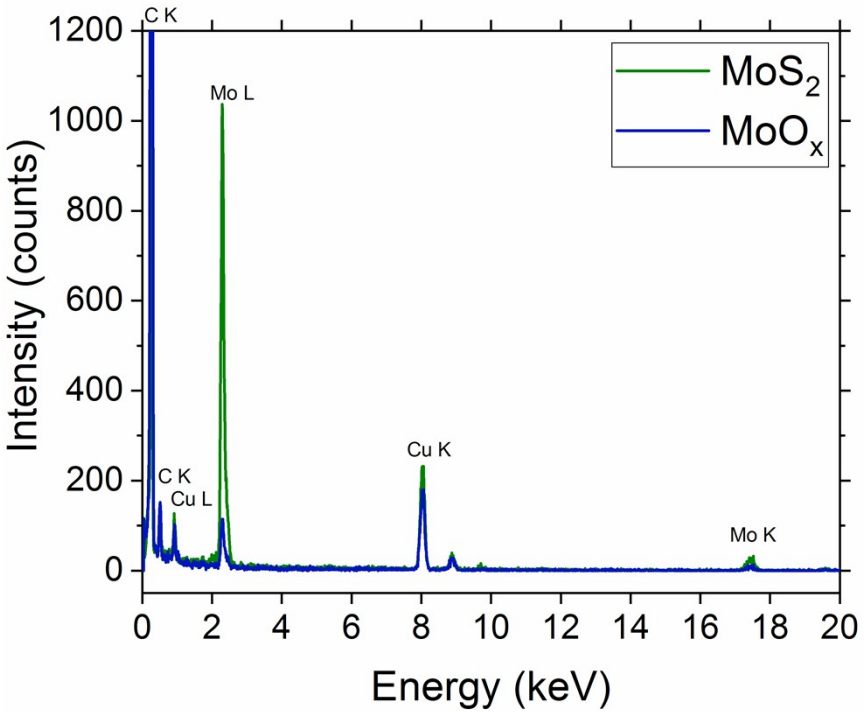

Fig. S23: EDS spectra of MoS_2 (prepared from 1 mg/ml) and MoO_x (prepared from 60 mg/ml) nanoparticles.

Singlet oxygen measurements

The EPR experiments were performed at ambient temperature (37 °C) using a Varian E-line spectrometer operating at a nominal frequency of 9.5 GHz. To follow the formation of singlet oxygen ($^1O_2$), 2,2,6,6-tetramethylpiperidine (TEMP) was used as a spin trap. TEMP molecules quickly react with $^1O_2$ and form a stable, EPR active product, TEMP-1O2 (TEMPO). For each MoO_x sample, 2 ml of MoO_x solutions were mixed with 90 µl of TEMP solution in ethanol. The prepared mixtures were exposed to blue light irradiation (P=15 W, t=12 h, λ=470 nm) at the temperature of 37 °C in the air-saturated environment. Aliquots (10 µl) of the TEMP solution from the control and the samples with an initial concentration of 20 mg/ml, 40 mg/ml and 60 mg/ml samples were then transferred into 2-3 mm (inner diameter) quartz tubes and the TEMPO signal was detected by EPR.

The concentration of generated singlet oxygen was estimated based on the creating (forming) of TEMPO which is produced during the photochemical reaction in the solutions. We calculated the integrated intensity of EPR spectrum of 2,2-diphenyl-1-picrylhydrazyl (DPPH) solution (at a concentration identical to MoO_x samples). An identical aliquot of 10 µl was used. The integrated intensity of EPR signals of TEMPO in each spectrum was calculated and divided by the value obtained for DPPH solution.

The production of singlet oxygen in MoO_x samples after a 12 h exposure to blue light was analyzed. The spin concentration of TEMP for the MoO_x samples are presented in Table S2. The sample with an initial concentration of MoS_2 of 60 mg/ml has one order of magnitude larger number of spins in comparison to the samples exfoliated from 20 mg/ml and 40 mg/ml solutions. The number of spins is directly proportional to the concentration of singlet oxygen produced by the nanoparticles. The EPR spectra of the individual samples are given in Fig. S24 – S29. We can see that intensities of characteristic EPR signals are much lower for the samples with initial concentrations of 20 mg/ml and 40 mg/ml compared to 60 mg/ml.

Table S2: The measured concentration of spin for MoO_x samples.

Initial concentration	Absolute concentration of spins
20 mg/ml	2.8×10^{14}
40 mg/ml	2.8×10^{14}
60 mg/ml	2×10^{15}

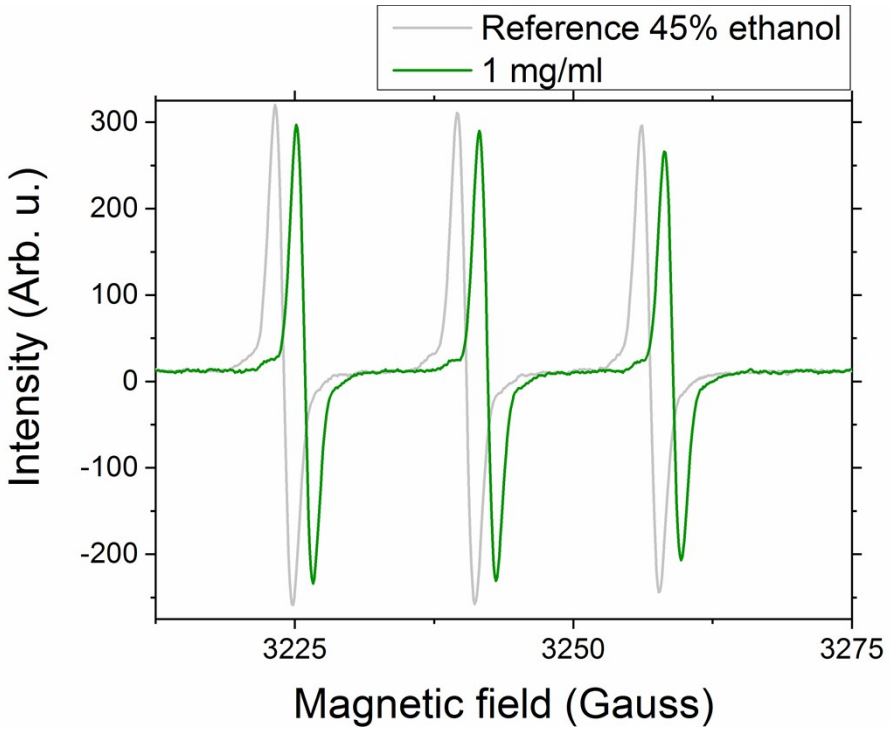

Fig. S24: The EPR spectrum of the irradiated sample prepared from an initial concentration of 1 mg/ml.

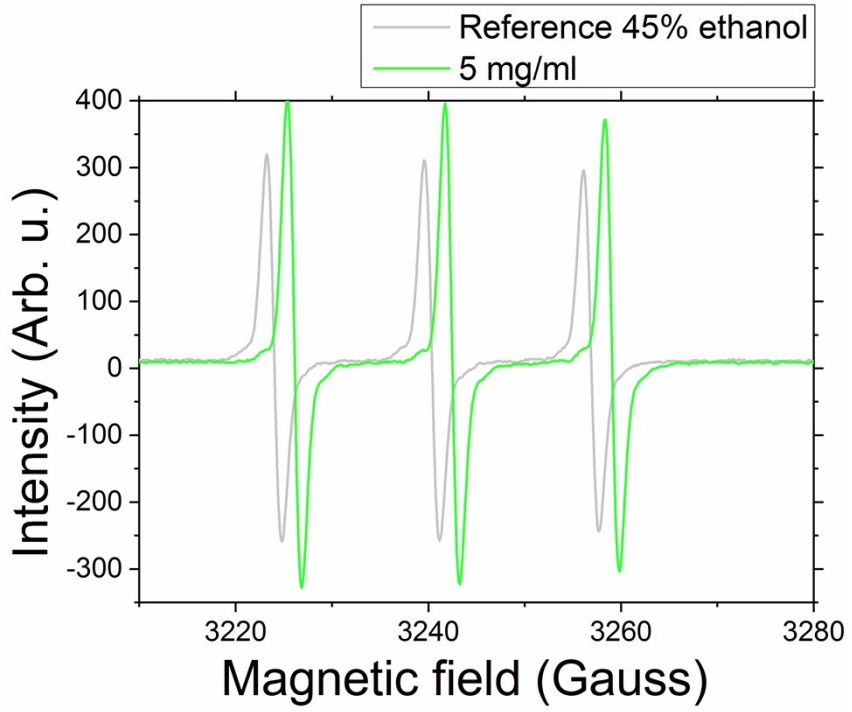

Fig. S25: The EPR spectrum of the irradiated sample prepared from an initial concentration of 5 mg/ml.

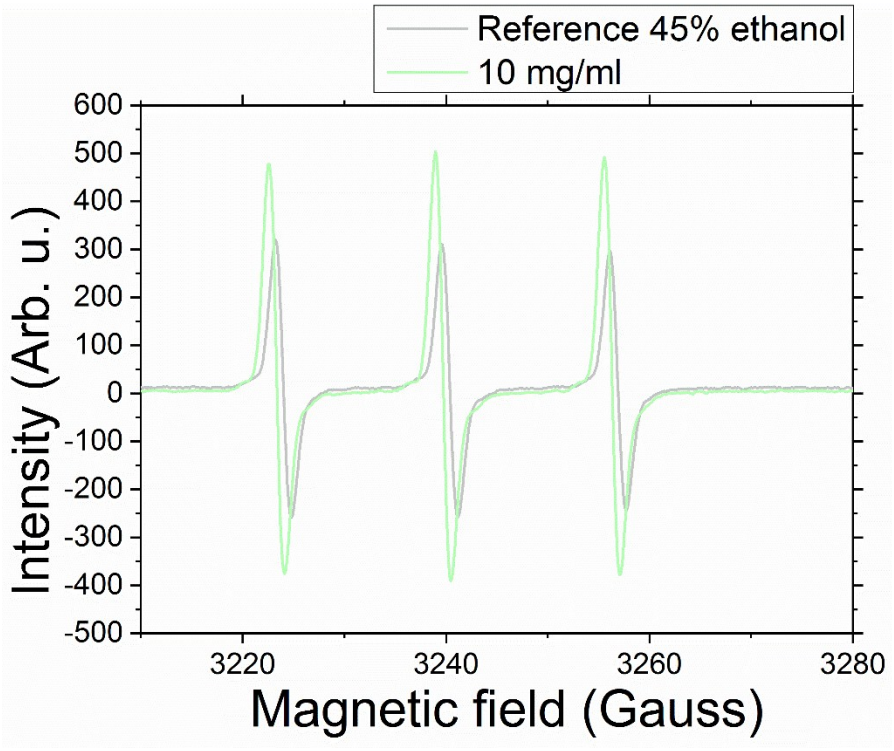

Fig. S26: The EPR spectrum of the irradiated sample prepared from an initial concentration of 10 mg/ml.

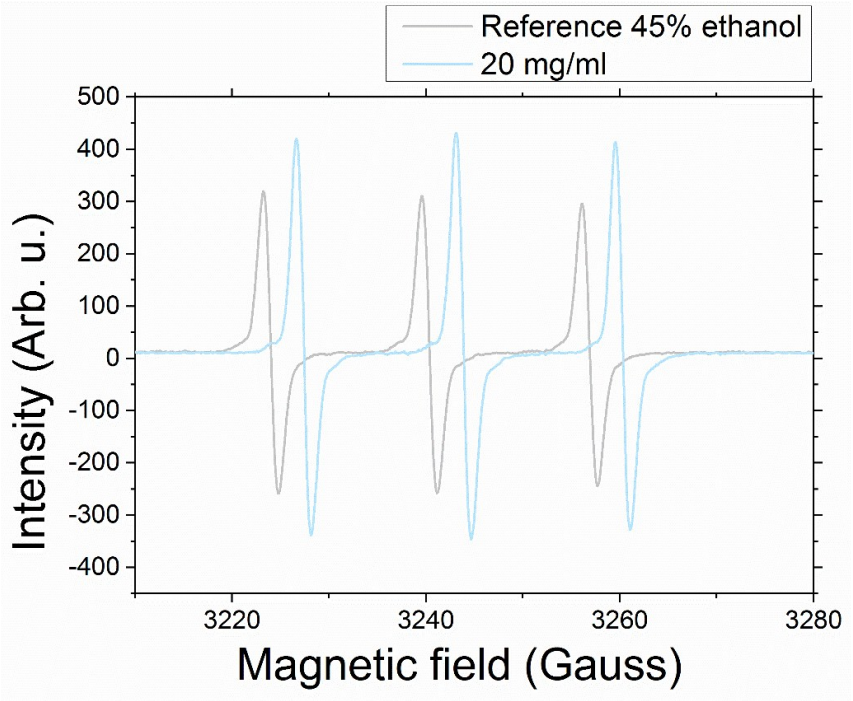

Fig. S27: The EPR spectrum of the irradiated sample prepared from an initial concentration of 20 mg/ml.

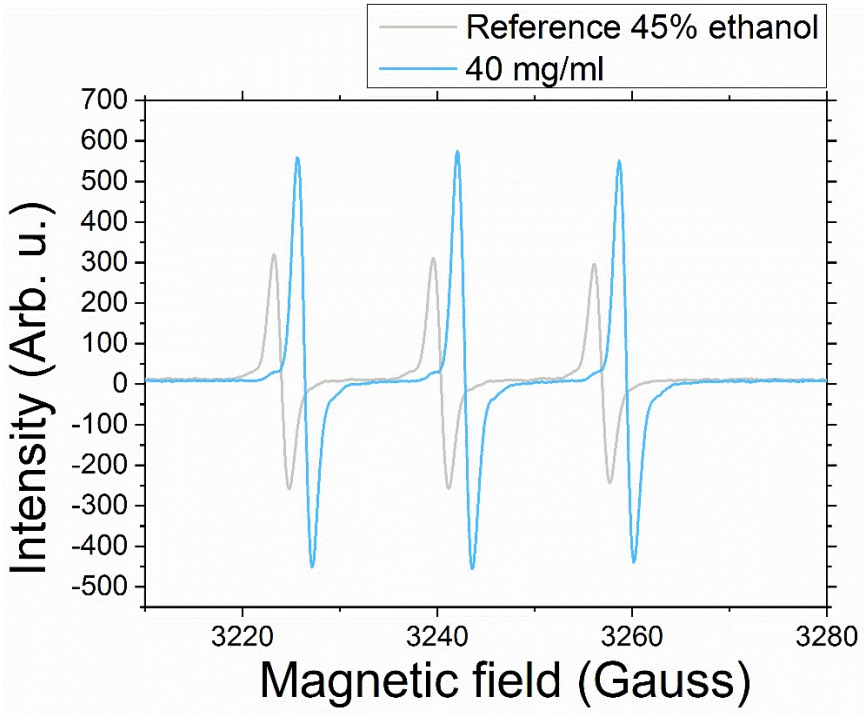

Fig. S28: The EPR spectrum of the irradiated sample prepared from an initial concentration of 40 mg/ml.

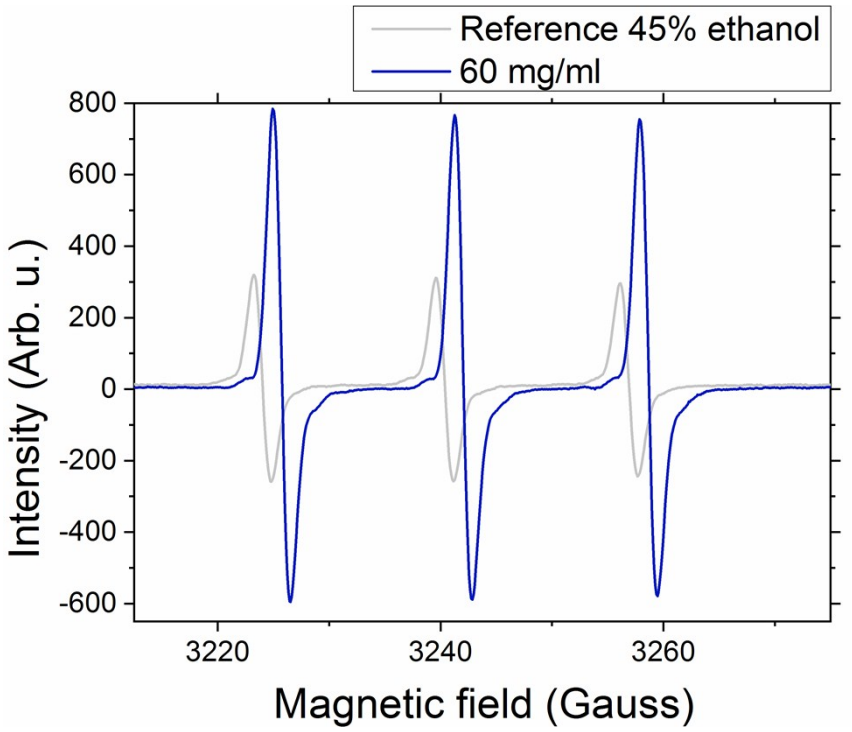

Fig. S29: The EPR spectrum of the irradiated sample prepared from an initial concentration of 60 mg/ml.

Titration curve

We measured the absorbance titration curves of all exfoliated products. The experiment was performed by successively changing the pH values followed by centrifugation and extraction of supernatant. The absorbance is directly related to the stability of solution at the given pH. The stronger the absorbance the more stable is the solution at the given pH. Fig. S30 shows the photography of the samples exfoliated from the 1 mg/ml MoS_2 concentration. The pH range spans from 1.61 on the left side to 11.47 on the right side. The photography (Fig. S31) of the MoO_x solutions (initial concentration 60 mg/ml) shows, that unlike the MoS_2 the MoO_x is stable in the given range of pH (1.73 – 10.77). This titration experiment points to the fact that the net surface charge of MoS_2 nanoflakes is negative. Moreover, this indicates that we cannot observe coexistence of both phases at low pH values (below 2.7).

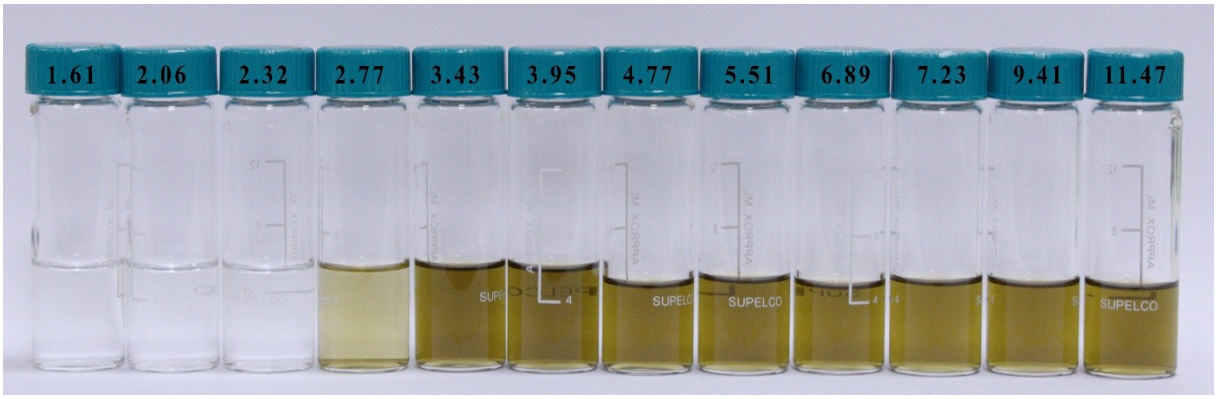

Fig. S30: The photography of MoS_2 samples with modified pH after centrifugation. The number indicates pH of the respective solution.

Fig. S31: The photography of MoO_x samples with modified pH after centrifugation. The number indicates pH of the respective solution.

Principal Component Analysis

The PCA was used to elucidate relations between individual samples taking into account correlation between the results of various experimental techniques. We used 24 different inputs, each input being one result from an analytical technique as a function of initial concentration of MoS_2. The area of an absorption peak, the PL intensity, etc. For the calculation, the correlation matrix method was employed. The first 7 of the total of 24 eigenvectors of PCA can explain 100% of the total variance (Table S3). The first two Principal Components (PC) were used to plot the scores of individual samples. In the two-dimensional PCA plot, the oxidation path of MoS_2 towards MoO_x follows roughly a straight line (Fig. S32). In Fig. S33 we plotted the identical data using the first three PCs, that describe almost 90% of all observed variations. In the landscape of three PCs, the oxidation path has a parabolic shape, while the exfoliated MoO_2 and MoO_3 samples are located in the opposite corner of the PC space suggesting their different behavior. The non-random parabolic oxidation path shows a correlation between the LPE MoS_2 samples suggesting that the oxidation is a progressive continuous process.

Table S3: The calculated eigenvalues corresponding to the first two PCs.

PC	Eigenvalue	Percentage of variance	Cumulative
1	13.41901	55.91%	55.91%
2	5.49297	22.89%	78.80%
3	2.5834	10.76%	89.56%
4	1.32658	5.53%	95.09%
5	0.58473	2.44%	97.53%
6	0.34075	1.42%	98.95%
7	0.25255	1.05%	100%
8	0	0%	100%

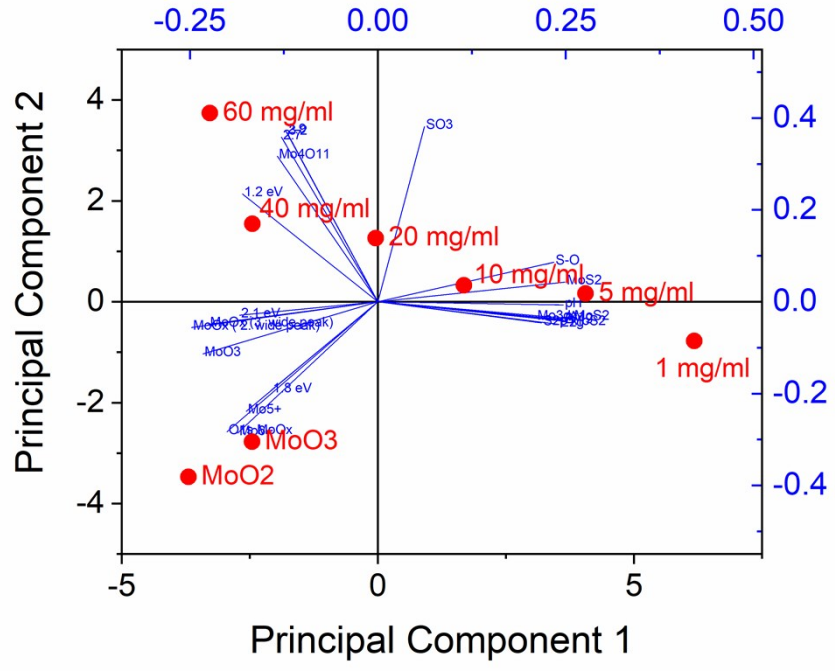

Fig. S32: The 2D PCA plot with the loading vectors.

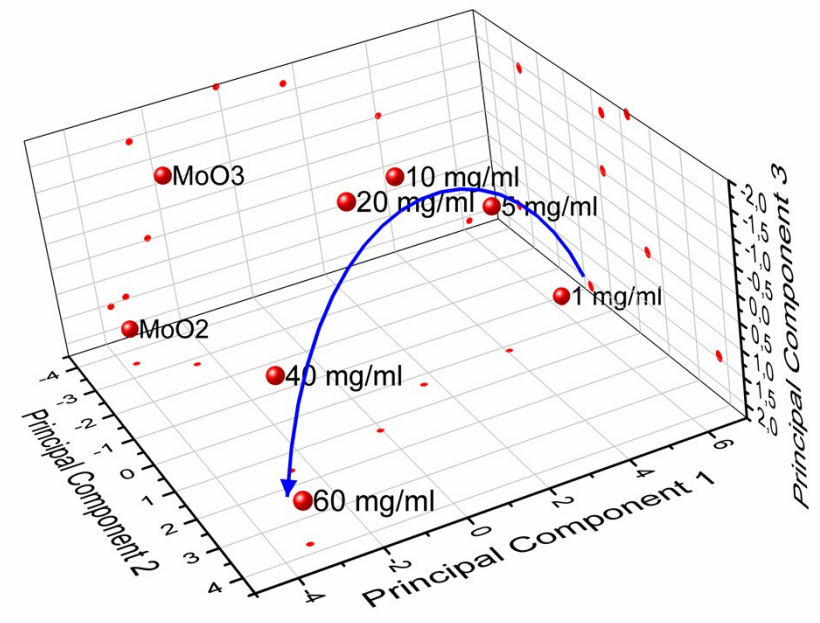

Fig. S33: 3D PCA plot using the first three PCs. The oxidation follows a parabolic path, while the final MoO_2 and MoO_3 exfoliated states are clearly offsite from this path. The small red dots are the projections of data points to individual planes.

Investigation of the reaction yield

The final concentration of MoO_x was determined by evaporating the sample prepared from 60 mg/ml of MoS_2 and weighting the precipitate. This way we determined the concentration in the solution prepared from 60 mg/ml and by subsequent dilution we prepared a set of samples for the calibration. Calibration curve (Fig. S34) was constructed from the absorbance of the samples at 1 000 nm.

Using this calibration curve, we could determine approximate concentration of the final product fraction directly from the absorbance measurement. The final concentrations of MoO_x solutions determined in this way showed, that the yield of MoO_x is increasing linearly with the increasing initial concentration of MoS_2 (Fig. S35). To reliably extrapolate the linear fit below 10 mg/ml initial concentration, we narrowed the confidence interval by using the fit of the

absorbance values at a wavelength of 1 000 nm (Fig. S36). The extrapolation shows, that the MoO_x starts to appear at the initial concentration of MoS_2 equal to 6 ± 2.5 mg/ml.

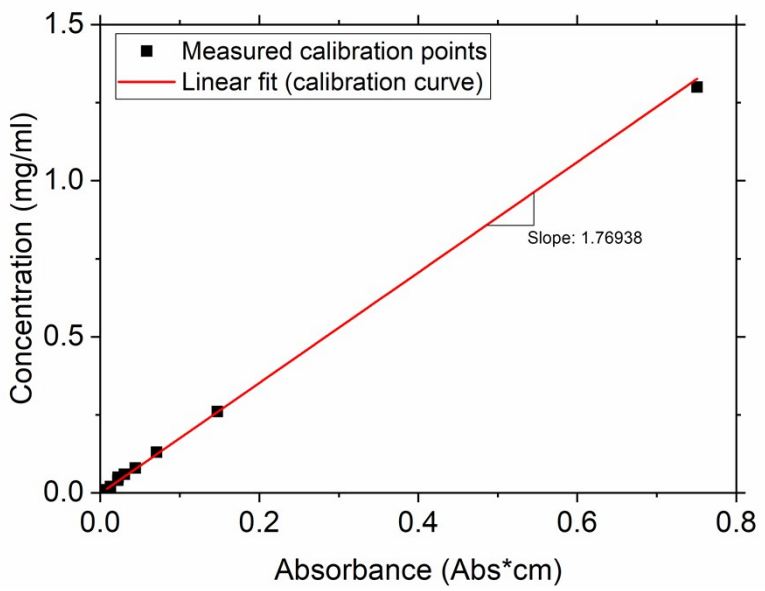

Fig. S34: Calibration curve for the determination of the MoO_x concentration.

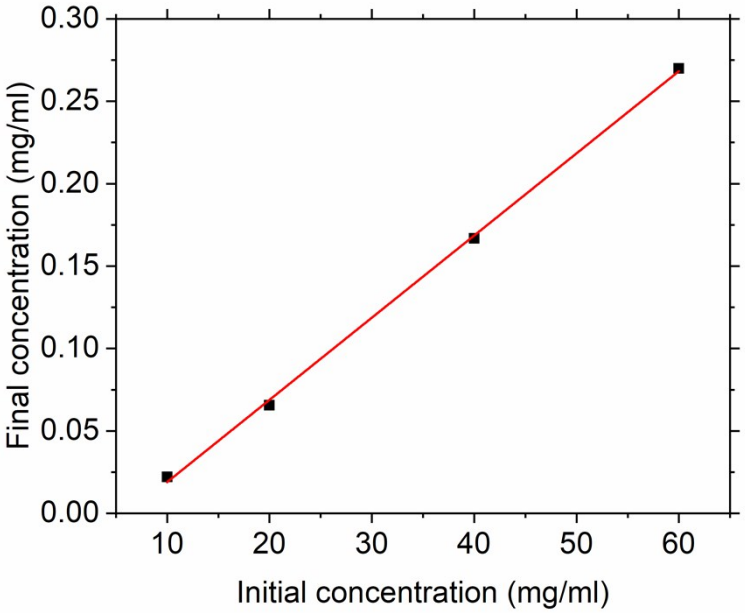

Fig S35: Final concentration of MoO_x as a function of the initial concentration of MoS_2 as determined from the absorbance.

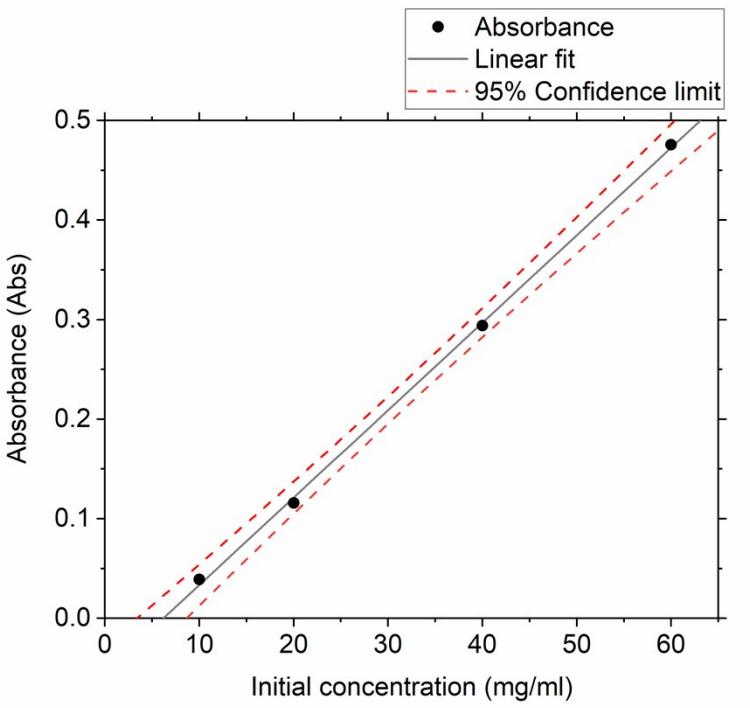

Fig. S36: The extrapolation of the absorbance of MoO_x peak showing the non-zero starting point.

The samples with the concentration close to the threshold point of the MoO_x production were prepared. We found that the presence of the MoO_x is already observable in the samples with the initial concentration larger than 5 g/ml (Fig. S37a). However, until the initial concentration is lower than 12.5 mg/ml the final product is present only in a small amount and the MoS_2 excitonic peaks are still dominating the absorbance spectra. After the initial concentration is raised above 12.5 mg/ml the final concentration of MoO_x is increasing linearly (Fig. S37b). Based on these findings, we can specify the threshold of initial concentration to be around 6.5 mg/ml. If the initial concentration is between 6 mg/ml and 12.5 mg/ml only a small amount of MoO_x is produced and the MoS_2 dominates the final product (Fig. 1). Further increase of the initial concentration over 12.5 mg/ml results in a stable production of MoO_x with a linearly increasing final concertation (Fig. S35, S37b).

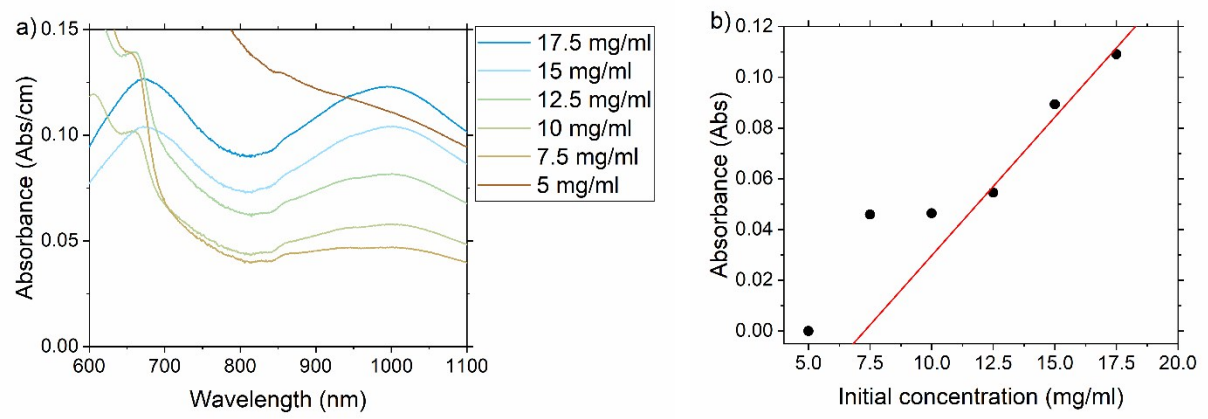

Fig. S37: a) The absorbance spectra of the samples with the initial concentration between 5 mg/ml and 17.5 mg/ml. b) The absorbance of the MoO_x peak at 1 000 nm showing a linear increase above the threshold concentration.

Preventing the oxidation

From our findings the neutralization of excessive charge before ultrasonication leads to an enhanced production of the exfoliated MoS_2 and effectively terminates its oxidation. To confirm this, we prepared two solutions with the initial MoS_2 concentration of 20 mg/ml. In the first case, the weighted MoS_2 was dissolved in the as-prepared 45% ethanol solution as usual. The pH of the as prepared solution was 3.0. In the second case, we altered the pH of the 45% ethanol solution using KOH. After we dissolved the MoS_2 powder in this solution, the pH of the resulting solution was 7.3. After the ultrasonication and centrifugation of both solutions, we obtained one product with the standard blue color of MoO_x. The second product with the altered pH resulted in a green MoS_2 solution (Fig. S38). This confirmed that the loss of MoS_2 is primarily due to a drop in the pH and a proper compensation of the additional charge can inhibit the oxidation.

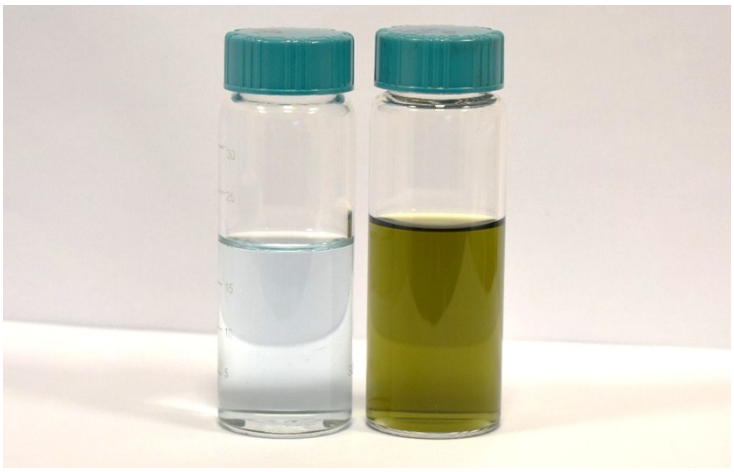

Fig. S38: The control experiment, where on the left the standard procedure was performed with the initial MoS_2 concentration of 20 mg/ml. On the right the same process was performed with the exception of additional charge compensation. The charge compensation resulted in the exfoliation of MoS_2 instead of its oxidation.